# KCNQ channels mediate $I_{Ks}$, a slow $K^+$ current regulating excitability in the rat node of Ranvier

J. R. Schwarz[1], G. Glassmeier[1], E. C. Cooper[2], T.-C. Kao[2], H. Nodera[3], D. Tabuena[3], R. Kaji[3] and H. Bostock[4]

[1] *Institute of Applied Physiology, University Hospital Hamburg-Eppendorf, University of Hamburg, Martinistr. 52, D-20246 Hamburg, Germany*
[2] *Department of Neurology, University of Pennsylvania, 409 Johnson Pavilion, 3610 Hamilton Walk, Philadelphia, PA 19104-6060, USA*
[3] *Department of Clinical Neuroscience, Graduate School of Medicine, University of Tokushima, 2-50-1 Kuramotocho, Tokushima City, 770-8503 Japan*
[4] *Sobell Department of Neurophysiology, Institute of Neurology, University College London, Queen Square, London WC1N 3BG, UK*

**Mutations that reduce the function of KCNQ2 channels cause neuronal hyperexcitability, manifested as epileptic seizures and myokymia. These channels are present in nodes of Ranvier in rat brain and nerve and have been proposed to mediate the slow nodal potassium current $I_{Ks}$. We have used immunocytochemistry, electrophysiology and pharmacology to test this hypothesis and to determine the contribution of KCNQ channels to nerve excitability in the rat. When myelinated nerve fibres of the sciatic nerve were examined by immunofluorescence microscopy using antibodies against KCNQ2 and KCNQ3, all nodes showed strong immunoreactivity for KCNQ2. The nodes of about half the small and intermediate sized fibres showed labelling for both KCNQ2 and KCNQ3, but nodes of large fibres were labelled by KCNQ2 antibodies only. In voltage-clamp experiments using large myelinated fibres, the selective KCNQ channel blockers XE991 ($IC_{50} = 2.2\ \mu M$) and linopirdine ($IC_{50} = 5.5\ \mu M$) completely inhibited $I_{Ks}$, as did TEA ($IC_{50} = 0.22$ mM). The KCNQ channel opener retigabine (10 $\mu$M) shifted the activation curve to more negative membrane potentials by −24 mV, thereby increasing $I_{Ks}$. In isotonic KCl 50% of $I_{Ks}$ was activated at −62 mV. The activation curve shifted to more positive potentials as $[K^+]_o$ was reduced, so that the pharmacological and biophysical properties of $I_{Ks}$ were consistent with those of heterologously expressed homomeric KCNQ2 channels. The ability of XE991 to selectively block $I_{Ks}$ was further exploited to study $I_{Ks}$ function *in vivo*. In anaesthetized rats, the excitability of tail motor axons was indicated by the stimulus current required to elicit a 40% of maximal compound muscle action potential. XE991 (2.5 mg kg$^{-1}$ I.P.) eliminated all nerve excitability functions previously attributed to $I_{Ks}$: accommodation to 100 ms subthreshold depolarizing currents, the post-depolarization undershoot in excitability, and the late subexcitability after a single impulse or short trains of impulses. Due to reduced spike-frequency adaptation after XE991 treatment, 100 ms suprathreshold current injections generated long trains of action potentials. We conclude that the nodal $I_{Ks}$ current is mediated by KCNQ channels, which in large fibres of rat sciatic nerve appear to be KCNQ2 homomers.**

(Resubmitted 2 February 2006; accepted after revision 2 March 2006; first published online 9 March 2006)
**Corresponding author** J. R. Schwarz: Institute of Applied Physiology, University Hospital Hamburg-Eppendorf, Martinistr. 52, D-20246 Hamburg, Germany. Email: schwarz@uke.uni-hamburg.de

In the mammalian node of Ranvier, $Na^+$ channels ($Na_v1.6$) are located at high density in the tiny stretch of the axolemma not covered by myelin, whereas the delayed rectifying $K^+$ channels (Kv1.1 and Kv1.2) are restricted to the juxta-paranodes (Poliak & Peles, 2003; Scherer *et al.* 2004). In addition to the $Na^+$ and fast $K^+$ current, a more slowly activating and deactivating $K^+$ current ($I_{Ks}$) has been observed in nodes of Ranvier. This current was first described in frog myelinated nerve fibres (Dubois, 1981). Indications for the existence of $I_{Ks}$ in mammalian nerve fibres and its function were later found by recording electrotonus in rat axons (Baker *et al.* 1987) and threshold electrotonus (the threshold analog of electrotonus) in humans (Bostock & Baker, 1988; Baker & Bostock, 1989). Subsequently, voltage-clamp experiments in single myelinated rat nerve fibres performed in isotonic KCl solution showed: that $I_{Ks}$, as in the frog node of Ranvier, starts to activate at membrane potentials as negative as −110 mV; that about 30% of $I_{Ks}$ is already activated at the resting potential; that it does not inactivate; and that it is almost totally blocked by 10 mM TEA (Röper & Schwarz, 1989; Safronov *et al.* 1993). The slow

 DOI: 10.1113/jphysiol.2006.106815

activation and deactivation kinetics of $I_{Ks}$ as well as the absence of inactivation were reminiscent of the M-current (Brown, 1988; Jentsch, 2000; Delmas & Brown, 2005), which was later shown to be mediated by heteromeric KCNQ2/KCNQ3 channels (Wang *et al.* 1998). Selective blockers of the M-current, like linopirdine and XE991 (Wang *et al.* 1998), and the M-current activator retigabine (Rundfeldt & Netzer, 2000; Wickenden *et al.* 2000; Tatulian *et al.* 2001), have greatly facilitated the analysis of M-currents.

Using immunohistochemistry, Devaux *et al.* (2004) recently demonstrated the existence of KCNQ2 and, in some cases, KCNQ3 subunit proteins at nodes of Ranvier in the rat sciatic nerve, spinal cord, and brain. In sciatic nerve fibres, KCNQ2 co-localized precisely with nodal $Na^+$ channels in the narrow unmyelinated part of the node of Ranvier. KCNQ3 proteins were also detected in these peripheral myelinated nerve fibres, but were not seen co-localized at the nodal membrane with KCNQ2 and $Na^+$ channels (Devaux *et al.* 2004). Instead, KCNQ3 antibodies labelled Schmidt-Lantermann incisures and outer mesaxons, portions of Schwann cell non-compact myelin involved in membrane–membrane contact.

The present experiments were performed to answer the question whether $I_{Ks}$ may be mediated by KCNQ channels and which function $I_{Ks}$ may have in peripheral nerve fibres. We show that in addition to the KCNQ2 channel protein, which is present in all nodes of Ranvier, the KCNQ3 channel protein can also be present in nodal membranes. However, the distribution and intensity of labelling for KCNQ3 channel proteins was dependent on fibre size; the occurrence of positive KCNQ3 staining drastically decreased in nerve fibres with large diameters. Voltage-clamp experiments performed in large single myelinated nerve fibres showed that $I_{Ks}$ could be blocked totally by XE991 or linopirdine, whereas it was activated by retigabine. Inhibition of $I_{Ks}$ by XE991 induced hyperexcitability in the isolated node of Ranvier. Using the threshold tracking method, we demonstrate a selective blockage of that component of threshold electrotonus which has been attributed to activation of $I_{Ks}$. In addition, the component induced by $I_{Ks}$ in the recovery cycle (Bostock *et al.* 1998; Burke *et al.* 2001) was blocked. Taken together, our experiments strongly suggest that $I_{Ks}$ is mediated by KCNQ channels and they demonstrate that selective blockage of $I_{Ks}$ by the KCNQ channel blocker XE991 induces a drastic increase in the ability of motor axons to fire repetitively.

## Methods

### Immunocytochemistry and microscopy

Rabbit anti-KCNQ2-N (anti-KCNQ2) antibodies were raised and affinity-purified as previously described (Cooper *et al.* 2001). These antibodies are directed against residues 13–37 from the intracellular N-terminal region of KCNQ2, which appear to be absolutely conserved in mammals (Singh *et al.* 1998; Pan *et al.* 2001). Guinea pig anti-KCNQ3b-N (anti-KCNQ3) antibodies (Devaux *et al.* 2004) are directed against residues 36–57 from the N-terminal region of splice isoforms of KCNQ3 using a longer first exon (Schroeder *et al.* 1998); this antibody does not recognize a splice isoform (KCNQ3a) that includes the shorter first exon (Wang *et al.* 1998). The $Na^+$ channel antibody used was $PanNa_v$ (clone K58/35, Sigma), a mouse monoclonal antibody against a peptide conserved in all voltage-gated $Na^+$ channel isoforms (Rasband *et al.* 1998). Secondary antibodies were purchased from Jackson Immunoresearch.

Adult male Wistar rats were killed by $CO_2$ inhalation and cervical dislocation. This method of killing was approved by the Institutional Animal Care and Use Committee of the University of Pennsylvania. Sciatic nerves were dissected and placed in cold phosphate-buffered saline solution. Fibres were teased out using fine needles, transferred to Superfrost Plus slides (Fisher), and allowed to air dry. Slides were stored at $-20^\circ$C overnight, or until used for staining with antibodies.

Antibody immunoreactions were performed essentially as previously described (Devaux *et al.* 2004). Briefly, unfixed nerves were permeabilized and extracted, and non-specific binding sites blocked by incubation with Tris-buffered saline solution containing 0.5% Triton X-100 and 5% fish skin gelatine for 1 h. Nerves were then incubated with primary antibody in blocking buffer (with 0.2% Triton X-100) for 15–18 h, washed, incubated with secondary antibodies for 2 h, washed, and coverslipped using ProLong antifade reagent (Molecular Probes). In all cases, multilabel experiments were performed in parallel with single label and secondary-only controls, which revealed no evidence of antibody cross-reactivity.

Fluorescence microscopy was performed using a Nikon TE2000 inverted microscope equipped with Chroma (31000, 41004 and 41017) filter sets and a $60 \times 1.4$ NA oil immersion objective. Monochrome images were acquired using a SPOT KE Slider cooled digital camera (Diagnostic Instruments). Colour superimpositions were performed and minimum and maximum intensity levels were adjusted using Photoshop (Adobe). Superimposition of fluorescence images and differential interference contrast (DIC) images were performed with the Photoshop add image function. Fibre diameters were determined using the measurement tool in SPOT image analysis software (Diagnostic Instruments), after calibration using a stage micrometer.

To quantify the percentage of nodes with and without associated KCNQ3 immunoreactivity, teased fibres were prepared from nerves of seven rats, and double-stained using mouse anti-$Na_v$ antibodies/FITC-conjugated

secondary antibodies, and guinea pig anti-KCNQ3 antibodies/Cy3 conjugated secondary antibodies. For ≥ 100 nodes per animal, the following procedure was performed: a node was selected at random on the basis of strong $Na_v$ (i.e. FITC) staining, and photographed. Then the filters of the microscope were changed and an image acquired of KCNQ3 (i.e. Cy3) stain. The images were superimposed in Adobe Photoshop, and the nodal KCNQ3 staining was classified as moderate or strong (e.g. Figs 2*I* and *L*, and 3*D*), weak/diffuse/glial (e.g. Figs 2*O* and 3*I*), or absent (e.g. Fig. 2*C* and *F*).

### Voltage- and current-clamp experiments

Male Wistar rats (250–350 g) were killed by exposure to $CO_2$ or by exposure to isoflurane with subsequent decapitation. These procedures were approved by the animal welfare committee of the University Hospital Hamburg-Eppendorf. Single myelinated nerve fibres were isolated from the sciatic nerve over a distance of two internodes by using fine needles, forceps (Dumont no. 5) and iridectomy scissors. The isolated nerve fibre was placed on top of the separating walls of the nerve chamber (see Fig. 1*A* and *B*) and fixed to the ridges with thin Vaseline seals. In addition to the electrical resistance provided by the Vaseline seals, the external resistance between pool B (connected to ground potential) and pool C was further increased by introducing an air gap (pool F in Fig. 1*B*). The side pools of the experimental chamber (Nonner, 1969) were filled with axoplasmic solution (see below) and both internodes were cut. A manually operated pulse generator and an oscilloscope were used for eliciting and monitoring of action potentials and membrane currents. After obtaining stable conditions, membrane currents and potentials were recorded by using the PULSE stimulation and data acquisition software (HEKA, Lambrecht) in

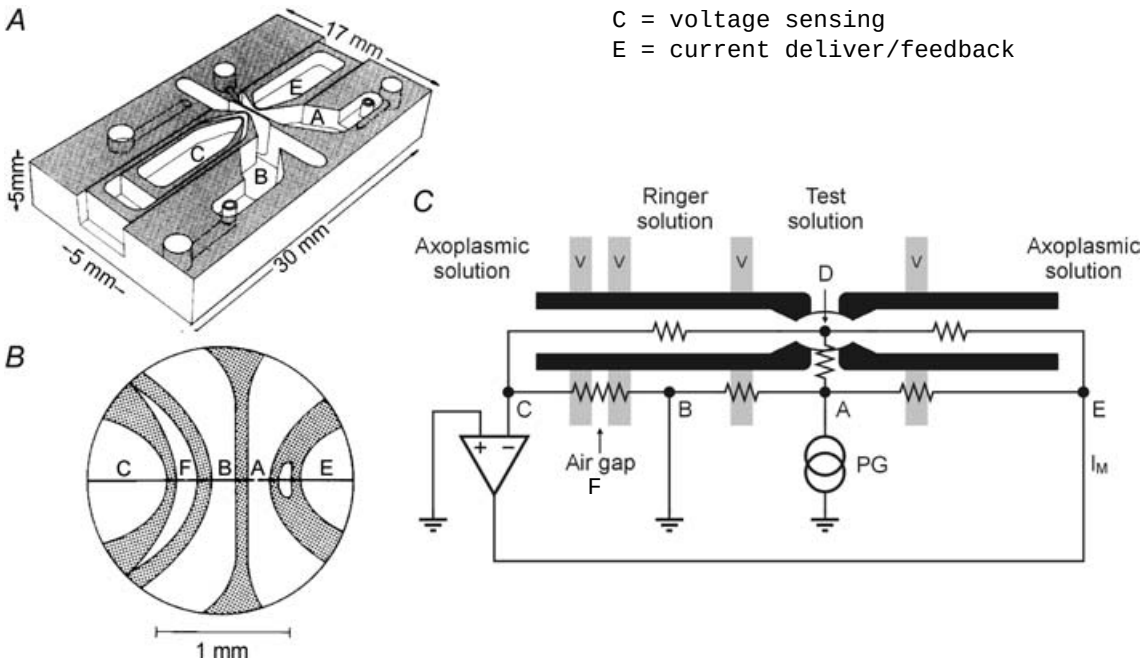


**Figure 1. Nerve chamber and schematic of voltage clamping the node of Ranvier**
*A*, nerve chamber for recording of action potentials and membrane currents of an isolated node of Ranvier. The nerve chamber is made of Perspex and consists of four compartments separated by thin walls. *B*, central part of the nerve chamber at higher magnification. A single nerve fibre is shown placed on top of the compartment ridges with the node of Ranvier located in the middle of compartment A. *C*, diagram demonstrating the principle of the voltage clamp (Nonner, 1969). E, A, B and C denote electrodes (designated corresponding to the compartments shown in panel *A*) in the fluid surrounding the nerve fibre. D, point in the axoplasm at the node. Vaseline seals (v) were placed on top of the ridges to increase the electrical resistance between the chamber compartments and to hold the fibre in position. F (in *B*) denotes an air gap to further increase the external resistance of the nerve fibre. After exchanging the solution in the side pools *C* and E for axoplasmic solution, the internodes of the nerve fibre under investigation were cut in both side pools. Therefore the electrodes in C and E were in direct contact with the axoplasm of the nerve fibre. PG, pulse generator. Input of the feedback amplifier connected with electrode C, its output connected with electrode E. For recording action potentials (current-clamp mode), the output of the amplifier was connected with electrode A and the pulse generator with electrode E. Modified from Stämpfli & Hille (1976).

conjunction with an EPC-10 patch-clamp amplifier. The measurements were performed at room temperature (20–23°C).

A schematic drawing of the method of Nonner (1969) of voltage clamping the node of Ranvier is shown in Fig. 1*C*. After cutting the internodes in both side pools the axoplasm of both internodes was in direct contact with the axoplasmic solution and the electrodes C and E. The feedback amplifier kept the potential at point C at ground potential by adjusting the potential at E. Any internodal current between C and D would also flow across the seal resistance between C and B and would produce a potential drop. The feedback amplifier prevented such a potential drop and thus eliminated flow of current between D and C. These two points were effectively kept at ground potential. The potential at A with respect to ground corresponded to the absolute membrane potential of the node under investigation. It could be changed by means of a pulse generator. By passing current through the resistance between E and D, the external potential in A was forced to follow the command waveform generated by the pulse generator. The current flowing between E and D was identical to the membrane current of the node under investigation and was recorded as the voltage drop across the resistance of the internode ED assuming an internodal resistance of 15 MΩ (for details see Nonner, 1969; Stämpfli & Hille, 1976; Neumcke *et al.* 1987; Röper & Schwarz, 1989). Membrane currents were low-pass filtered at 3 kHz. Capacity currents and leakage currents were not subtracted. At the beginning of each experiment, the holding potential ($E_H$) was adjusted so that about 30% of the $Na^+$ current was inactivated ($h_\infty = 0.7$). In most experiments the node was superfused with isotonic KCl, so that $E_H$ was determined from the potential step required to reach the reversal potential for $K^+$, assuming $E_K = 0$ mV. The value of $E_H$ measured in this way was $-75.1 \pm 1.3$ mV (mean ± S.E.M.; $n = 18$). A similar value for the resting potential was previously reported for rat nerve fibres: −80 mV (Brismar, 1980), −78 mV (Neumcke & Stämpfli, 1982) and −77 mV (Röper & Schwarz, 1989). A value of −75 mV was used to determine the absolute membrane potential in those fibres in which $E_K$ was unknown.

The following solutions (mM) were used: Ringer solution: NaCl 154, KCl 5.6, $CaCl_2$ 2.2; isotonic KCl: KCl 160, $CaCl_2$ 2.2; axoplasmic solution: KCl 160. The pH was adjusted to 7.4 with Tris-HCl. All chemicals were purchased from Sigma, and XE991 from Tocris, Ellisville. Additional batches of XE991 as well as retigabine were a kind gift of Dr D. Isbrandt (ZMNH, University of Hamburg).

### *In vivo* experiments

Male Wistar rats (250–300 g) were anaesthetized with ketamine (30 mg kg$^{-1}$ I.P.) and xylazine (10 mg kg$^{-1}$ I.P.). In addition, diazepam (2 mg kg$^{-1}$ I.P.) was administered to prevent convulsions occurring after administration of XE991 (1–5 mg kg$^{-1}$ I.P.). The animal welfare committee of the University of Tokushima agreed to this procedure. The anaesthetized rats were placed on a warming mat to maintain a temperature between 32 and 35°C. Ag–AgCl disk electrodes (15 mm in diameter) were used for stimulation. The cathode was attached to the lateral aspect of the tail at 15 mm from the base. The anode was placed on the skin of the hip where the hair was removed. Stainless needle electrodes were used for recording compound muscle action potentials and for ground. The recording electrode was inserted into the ipsilateral aspect of the tail muscle 60 mm distal to the stimulating electrode and the reference electrode was placed 20 mm distal to the recording electrode. A ground electrode was placed in between the stimulating and recording electrodes, 20 mm proximal to the recording electrode (for details see Yang *et al.* 2000). Stimulation was controlled by a PC running Qtrac software (Institute of Neurology, London), connected via a Micro 1401 data acquisition unit (Cambridge Electronic Design, Cambridge, UK) to the electromyogram preamplifier (Nihon Kohden MEG-1200) and stimulator (purpose-built ±50 mA bipolar voltage–current converter).

Using 1 ms rectangular stimuli and recording the negative peak of the compound muscle action potential, the excitability tests entailed first recording the stimulus–response curve, and then using the slope of the curve to track the stimulus required to evoke a 40% of maximal response, which was defined as the 'threshold' stimulus. To record threshold electrotonus, one Qtrac channel tracked the unconditioned threshold, while four other channels determined the threshold at discrete points during and after 100 ms polarizing currents, set to ±20% and ±40% of the unconditioned threshold. The five Qtrac channels were activated in turn, one every 0.8 s (see Kiernan *et al.* (2000) for a more complete description of the method). To record the recovery cycle, the unconditioned threshold was again tracked continuously on one Qtrac channel, while on another channel a supramaximal conditioning stimulus was given at 18 delays from 200 ms to 2 ms before the test stimulus. To separate the responses to conditioning and test stimuli when they overlapped, the response to the conditioning stimulus alone was recorded on a separate channel and subtracted from the response to the double stimulus. To track the recovery cycle following a short train of impulses, two more channels were used to record the effects of a train of seven supramaximal conditioning stimuli at 4 ms intervals, with the last conditioning stimulus delivered between 200 and 2 ms before the test stimulus. In some experiments, an additional Qtrac channel was used throughout the recording period to deliver a 100 ms current pulse equal in amplitude to the (1 ms) threshold

current. For this stimulus, all the muscle action potentials above the noise level were recorded, to provide a measure of the tendency of the depolarized motor axons to fire repetitively.

## Results

### Immunocytochemistry

KCNQ2 and KCNQ3 subunit proteins were localized in teased fibres from sciatic nerve using polyclonal antibodies against the two channel proteins. Nodes were identified by co-labelling fibres with a mouse monoclonal antibody against voltage-gated $Na^+$ channels, $PanNa_v$. Strong KCNQ2 and $Na^+$ channel immunoreactivity were always co-localized in narrow $\sim$1 $\mu$m patches along the fibres, i.e. the nodes, and were absent from internodes and myelin (Fig. 2*A* and *B*). At some nodes, labelling for KCNQ2 and $Na^+$ channels appeared as parallel lines, suggestive of membrane localization.

KCNQ3 immunoreactivity was much more widely distributed along the nerve fibres and, unlike immunoreactivity for KCNQ2 and $Na^+$ channels, was also detected at outer mesaxons and incisures, which are locations representing sites of membrane–membrane adhesion and contact in the myelin sheath (as previously noted, Devaux *et al.* 2004). However, node-like clusters of KCNQ3 immunoreactivity were detected in teased nerve samples singly labelled with anti-KCNQ3 antibodies. To determine if these were nodes, we performed double label experiments using KCNQ3 antibodies and either KCNQ2 (Fig. 2*A–C* and *G–I*) or $Na^+$ channel (Fig. 2*D–F* and *J–O*) antibodies. The results were strikingly variable. Some nodes exhibited a complete absence of KCNQ3 immunoreactivity at characteristic KCNQ2 or $Na^+$ channel node-like clusters (Fig. 2*A–F*). Others exhibited strong KCNQ3 immunoreactivity that was well co-localized with the nodal markers (Fig. 2*G–L*). A third category of fibres exhibited an intermediate intensity of nodal staining, that was often accompanied by more intense labelling of outer

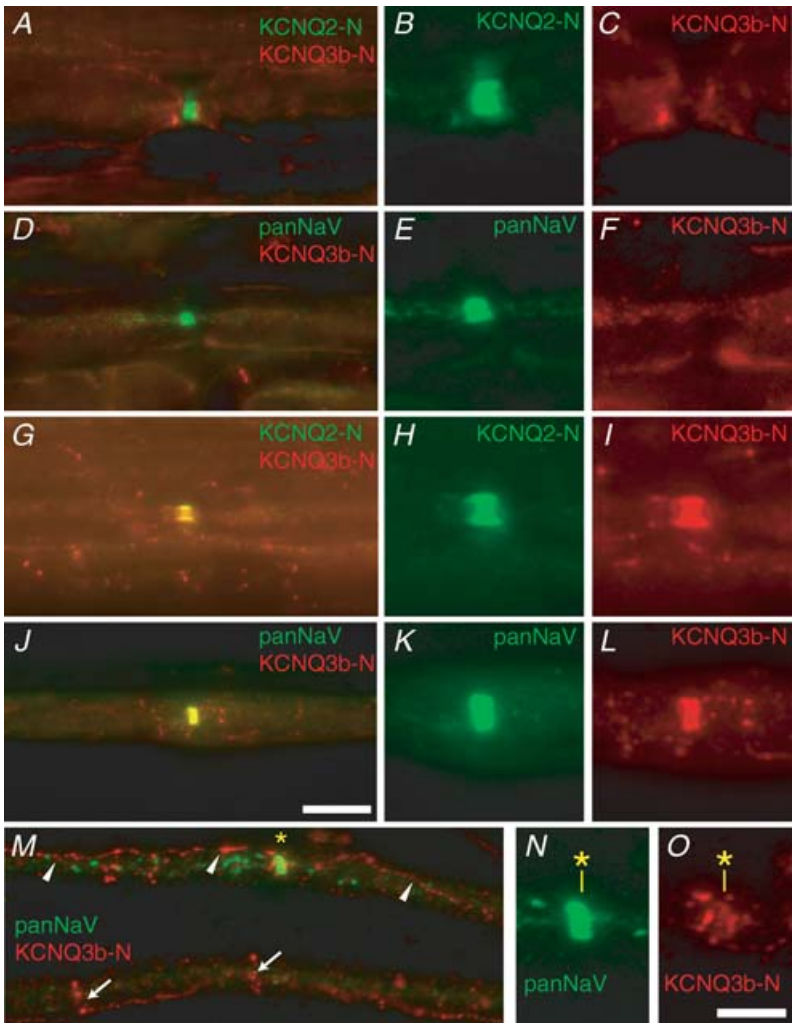


**Figure 2. KCNQ2 is strongly localized to nodes of rat sciatic nerve fibres, but KCNQ3 exhibits a heterogeneous distribution**
*A–F*, fibres show strong KCNQ2 or $Na^+$ channel labelling at nodes, but absence of nodal KCNQ3 immunoreactivity. Fibres were labelled with rabbit anti-KCNQ2-N or mouse $panNa_V$, and guinea pig anti-KCNQ3b-N antibodies, and primary antibodies were detected using FITC-donkey anti-rabbit or anti-mouse and Cy3 donkey anti-guinea pig secondary antibodies. *A*, lower power image showing KCNQ3 (red) labelling of myelin and KCNQ2 (green) labelling of node. *B* and *C*, nodal region at higher power, with strong KCNQ2 staining of the node, but no co-labelling for KCNQ3. *D–F*, similar images as *A–C*, but double labelled for $Na^+$ channels and KCNQ3. *G–L*, representative images, acquired as described for *A–F*, illustrating nodes apparently positive for KCNQ3b-N. In some examples (i.e. panel *I*), the KCNQ3b-N immunoreactivity is not only highly concentrated at the node, but exhibits a parallel line distribution suggestive of membrane labelling. *M–O*, some fibres show a combination of strong myelin labelling and weak nodal labelling for KCNQ3. *M*, two fibres conspicuously labelled by KCNQ3 antibodies at outer mesaxons (arrowheads) and incisures (arrows), as described by Devaux *et al.* (2004). A node is strongly labelled by $panNa_V$ antibodies only (*). *N* and *O*, higher power images showing that strong $panNa_V$ staining of the node is associated with strong punctate KCNQ3b-N staining around the node, and weaker but detectable KCNQ3b-N staining at the node itself. Scale bars, 10 $\mu$m (*A*, *D*, *G*, *J* and *M*) and 5 $\mu$m (*B*, *C*, *E*, *F*, *H*, *I*, *J*, *K*, *L*, *N* and *O*).

mesaxons, incisures and punctate staining near, but not at the node itself (Fig. 2*M–O*). We quantified these results on teased fibres prepared from seven animals. For each set of fibres, KCNQ2 or $Na^+$ channel node-like clusters were selected randomly and photographed using a high-power objective, and then the pattern of KCNQ3 nodal immunoreactivity was determined. KCNQ3 immunoreactivity was strong in $23 \pm 14\%$, weak or most conspicuously glial in $27 \pm 9\%$, and absent in $50 \pm 16\%$ of the nodes ($n = 702$, mean $\pm$ S.D.).

The fibre composition of rat sciatic nerve is heterogeneous, including about 8000 myelinated motor and sensory fibres that vary in size, pharmacological sensitivity, and such physiological properties as conduction velocity and frequency adaptation (Schmalbruch, 1986; Gokin *et al.* 2001; Vleggeert-Lankamp *et al.* 2004). To learn whether the variability in KCNQ3 staining pattern we observed might be correlated with functional differences among nerve types, we performed an additional analysis of KCNQ3 localization as a function of myelinated fibre diameter. We visualized teased, immunostained fibres with a combination of DIC and fluorescence optics (Fig. 3). DIC images revealed bleb-like distortion of the myelin structure in these unfixed detergent-treated fibres, most clearly near the nodes, which in many cases appeared partially demyelinated for a distance of about 5 $\mu$m (Fig. 3*B* and *G*). We measured the cross-sectional diameter of well-isolated single fibres in DIC images, and classified the pattern of KCNQ3 immunostaining as previously. Again, the fibres exhibited a mixture of absent (data not shown), strong and often nodal membrane associated (Fig. 3*A–E*), and weak/diffuse/glial (Fig. 3*F–H*) KCNQ3 patterns. However,

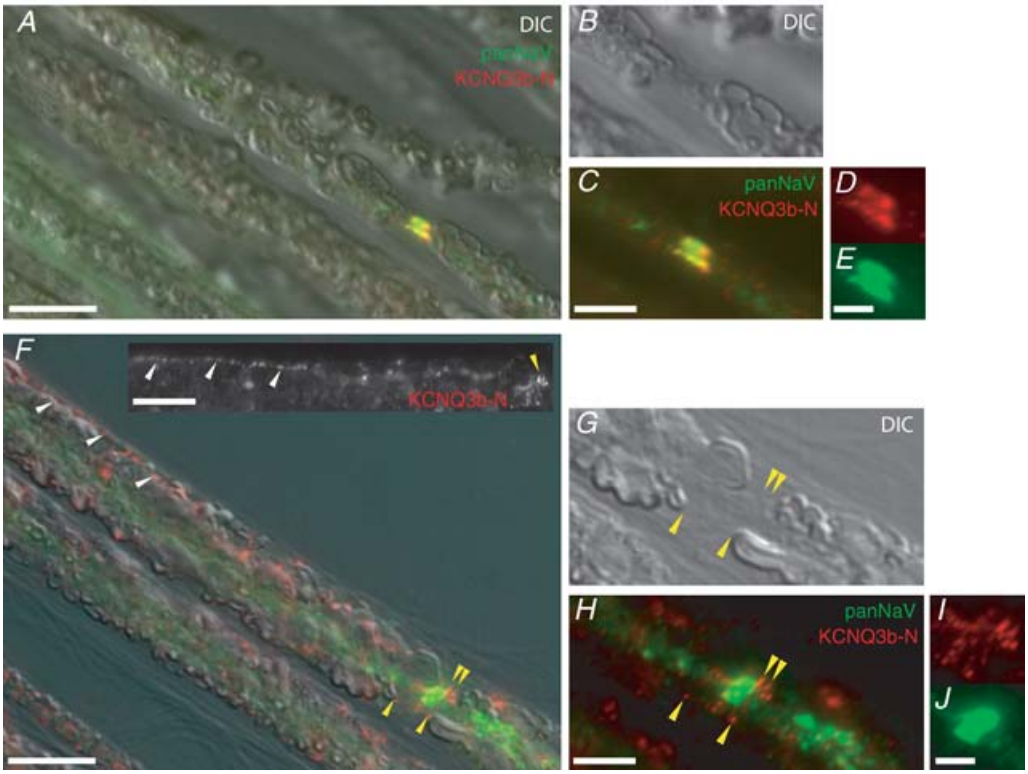


**Figure 3. Larger diameter fibres are less likely to exhibit nodal KCNQ3 immunostaining**
*A–E*, a 3 $\mu$m diameter fibre exhibits strong nodal membrane co-labelling by panNa$_V$ and KCNQ3b-N antibodies. *A,* lower magnification DIC image of several myelinated fibres, with superimposed panNa$_V$ (green) and KCNQ3b-N (red) immunostaining at a node. *B*, DIC image of the nodal region from panel *A,* showing the bleb-like appearance of myelin membranes and demyelination near the node. *C*, immunofluorescence image of identical region to *B*, showing colabelling of nodal membrane by $Na^+$ channel and KCNQ3b-N antibodies. *D, E,* pattern of KCNQ3b-N (*D*, red) and $Na^+$ channel (*E*, green) immunoreactivity at the same node. *F–J*, a 10 $\mu$m fibre showing conspicuous labelling of glial membranes and puncta near the node, but weak nodal labelling. *F*, lower magnification image showing fibre with puncta of KCNQ3 staining along its length (white arrowheads), and near the node (yellow arrowhead), and strong Na channel labelling of the node. Inset shows KCNQ3 immunostaining along axon in grey scale; the arrowheads indicate an apparent labelled outer mesaxon. *G, H*, DIC and immunofluorescence images of nodal regions reveal strong nodal panNa$_V$ stain and puncta of KCNQ3b-N staining near the node. Several KCNQ3-immunoreactive puncta appear to be localized at tips of glial blebs near the node (yellow arrowheads). *I, J*, individual colour channels showing pattern of KCNQ3 (*I*, red) and $Na^+$ channel (*J*, green) immunoreactivity at node. Scale bars, 10 $\mu$m (*A, F*), 5 $\mu$m (*B, C, G, H*), and 2.5 $\mu$m (*D, E, I, J*).

smaller fibres (2–6 $\mu$m) were more likely to exhibit strong nodal KCNQ3 staining than medium fibres (7–9 $\mu$m), and this sampling revealed no large fibres of 10 $\mu$m or greater with strong KCNQ3 immunoreactivity at the node (Fig. 4).

### Voltage- and current-clamp experiments

**Membrane currents.** Large single myelinated nerve fibres were isolated from the rat sciatic nerve, mounted in the experimental chamber, and action potentials and membrane currents were recorded using the experimental set-up described in Methods (Nonner, 1969; Stämpfli & Hille, 1976; Schwarz *et al.* 1995). The holding potential was adjusted to the membrane potential at which 30% of the $Na^+$ channels were inactivated ($h_\infty = 0.7$), i.e. about −75 mV (see Methods). Since in Ringer solution the amplitude of $I_{Ks}$ currents was very small and $I_{Ks}$ had to be isolated from the other currents with XE991, it was not possible to measure accurately in Ringer solution properties of the current such as the time course of activation and deactivation. Therefore, as was previously done by Dubois (1981) and Röper & Schwarz (1989), most of the voltage-clamp measurements were performed in isotonic KCl solution to increase the $I_{Ks}$ amplitude. $Na^+$ currents were not detected under these recording conditions (external and axoplasmic solutions did not contain $Na^+$), therefore tetrodotoxin was not added to the test solutions. Upon exchanging Ringer to isotonic KCl solution a steady inward current appeared at the holding potential of −70 mV (Fig. 5*A*). Upon a potential step to −130 mV a tail current was elicited which, after a short delay, slowly deactivated to reach a small constant inward current. Upon repolarization to the holding potential, the initial current amplitude was almost zero; thereafter the inward current slowly increased to reach the level of the holding current which was the same as before applying the negative potential step. Figure 5*A* shows superimposed membrane currents recorded with 80 ms potential steps varying between −130 and 50 mV. Upon application of 100 $\mu$M XE991, the holding current as well as a large part of the currents recorded upon the hyperpolarizing test pulses were blocked. The currents elicited upon depolarizing pulses were also reduced. The XE991-sensitive current (obtained by subtracting the current traces recorded in the presence of the inhibiting substance from the corresponding control current traces) clearly showed that XE991 totally blocked $I_{Ks}$. The membrane currents remaining unblocked by XE991 consisted of XE991-insensitive $K^+$ currents and an unspecific leakage current. The leakage current in the node of Ranvier is that current component exhibiting a linear voltage dependence (see Fig. 2 in Röper & Schwarz, 1989; see also Stämpfli & Hille, 1976). The XE991-sensitive current (Fig. 5*C*) had the same properties as $I_{Ks}$ described by Dubois (1981) in frog and by Röper & Schwarz (1989) in rat nerve fibres: it was already activated at the holding potential of −70 mV, upon negative and positive potential steps it slowly deactivated and activated in a potential-dependent way, and it did not inactivate. The voltage dependence of $I_{Ks}$ activation was determined from the tail current amplitudes of the XE991-sensitive current recorded upon repolarization to the holding potential (Fig. 5*C*). The tail current amplitudes were normalized to the maximal tail current and plotted *versus* test pulse potential. Fifty per cent of $I_{Ks}$ was activated at $E_{0.5} = -61.7 \pm 1.4$ mV (mean ± S.E.M.; $n = 11$), the slope factor being 12.3 ± 0.8 mV. This value was similar to the value of −60 mV measured by Röper & Schwarz (1989) in the rat and by Dubois (1981) in the frog, and similar to the values for $E_{0.5}$ obtained with the patch-clamp technique in rat (−76 mV, Safronov *et al.* 1993) and human nerve fibres (−68 mV, Reid *et al.* 1999). The latter experiments have also been done in isotonic KCl solution. As shown below, the voltage dependence of $I_{Ks}$ activation was remarkably sensitive to the external $K^+$ concentration ($[K^+]_o$).

**Pharmacology of $I_{Ks}$.** It has been reported that 50% of the native M-current recorded in supracervical ganglion cells was blocked by 0.98 $\mu$M XE991 and 50% of the current mediated by homomeric KCNQ2 or heteromeric KCNQ2/3 channels after heterologous expression in CHO cells was blocked by 0.71 and 0.6 $\mu$M XE991, respectively (Wang *et al.* 1998). To determine the concentration-dependent inhibition by XE991 of the nodal $I_{Ks}$, the current recorded in the presence

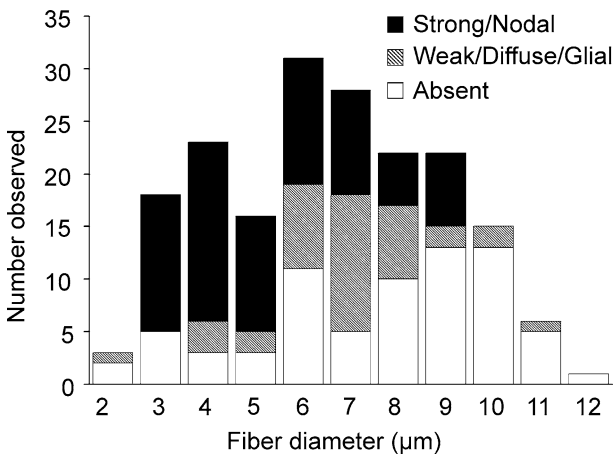


**Figure 4. KCNQ3 staining pattern depends on fibre diameter**
Bar graph showing the dependence of KCNQ3 staining pattern on fibre diameter. Smaller fibres had a higher likelihood of showing a strong KCNQ3 nodal staining; the largest fibres most often show glial staining, accompanied by weak, diffuse or absent KCNQ3 staining at the node.

of 100 $\mu$M XE991 was assumed to represent 100% $I_{Ks}$ inhibition. This current was subtracted from the current traces recorded at lower XE991 concentrations. The amplitudes of these tail currents were normalized and plotted against the XE991 concentration. A Hill function fitted to the data points yielded a 50% inhibition of $I_{Ks}$ by 2.2 $\mu$M XE991, the Hill coefficient being 1.2 (Fig. 6*A*). Similar experiments were performed with linopirdine, another substance used to block KCNQ-mediated currents. Linopirdine at 100 $\mu$M totally blocked $I_{Ks}$. There was no additional block of the remaining membrane current by subsequent application of 100 $\mu$M XE991. Fifty per cent of $I_{Ks}$ was blocked by 5.5 $\mu$M linopirdine, the Hill coefficient being 1.0 (Fig. 6*B*).

Previously, 10 mM TEA was used to block $I_{Ks}$ in voltage-clamped nodes of Ranvier (Röper & Schwarz, 1989) or 1 mM TEA to block $I_{Ks}$ in rat dorsal root fibres (Baker *et al.* 1987). Since it has been shown that the current mediated by homomeric KCNQ2 channels is much more sensitive to TEA ($IC_{50}$ = 0.16 mM; Wang *et al.* 1998) than that mediated by heteromeric KCNQ2/3 channels ($IC_{50}$ = 3.5 mM; Wang *et al.* 1998) we determined the dose–response curve of TEA. The reduction of the slow component of the tail current recorded upon repolarization to −70 mV after superfusion with increasing concentrations of TEA was determined, normalized to the maximal tail current amplitude and plotted *versus* the TEA concentration. The Hill function fitted to the data yielded an $IC_{50}$ of 0.22 mM TEA (Fig. 6*C*). This value is much closer to the TEA concentration needed to block homomeric KCNQ2 channels than to that needed to block heteromeric KCNQ2/3 channels (Wang *et al.* 1998). Since it is much more difficult to dissect rat nerve fibres of small diameter as compared with those of large diameter, only large diameter nerve fibres were investigated. The high sensitivity of these nodes to TEA nicely corresponds to the immunohistochemical finding that large fibres predominantly stain only for KCNQ2 channel proteins. These results together with the $E_{0.5}$ value of the activation curve suggested that in the rat node of Ranvier of large nerve fibres the channels mediating $I_{Ks}$ may predominantly be formed by KCNQ2 channel subunits only.

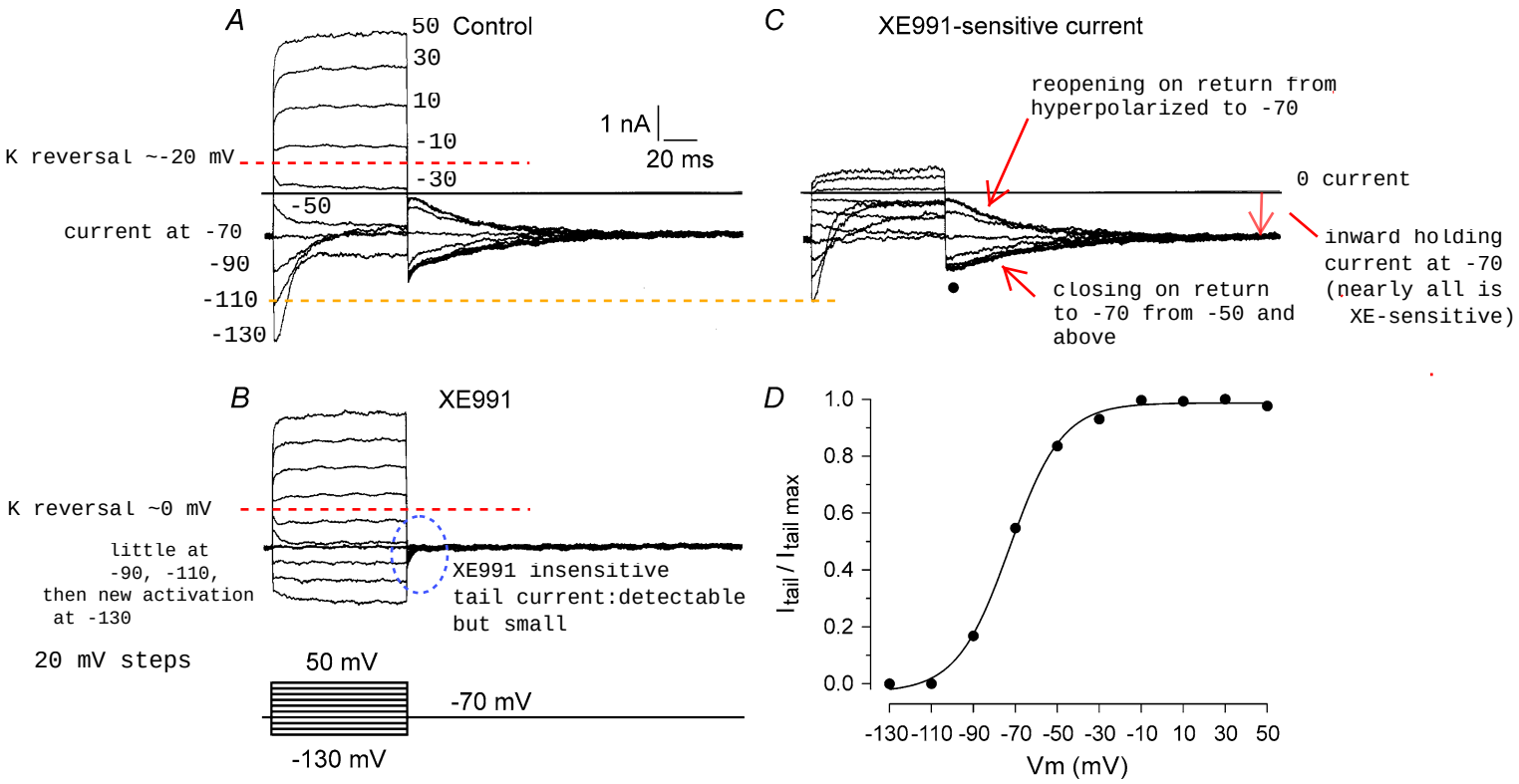


**Figure 5. XE991-sensitive current measured in isotonic KCl**
*A–C*, membrane currents recorded in isotonic KCl. Holding potential, −70 mV. Hyperpolarizing and depolarizing potential steps (duration, 80 ms) were applied before (*A*, Control) and after application of XE991 (100 $\mu$M; *B*) in steps of 20 mV. Subtraction of the membrane current traces shown in *B* from those in *A* yielded the XE991-sensitive current (*C*). *D*, activation curve, determined from the normalized amplitude of the tail currents recorded upon repolarization to the holding potential plotted against the amplitude of the preceding test pulses. A Boltzmann equation was fitted to the data points yielding $E_{0.5}$ = −72 mV (slope factor $k$ = 12.5 mV).

Retigabine has been shown to increase the amplitude of the M-current as well as heterologously expressed KCNQ currents by shifting the activation curve to more negative membrane potentials (Rundfeldt & Netzer, 2000; Wickenden *et al.* 2000; Tatulian *et al.* 2001). We were therefore interested to investigate whether retigabine has similar effects on $I_{Ks}$. In the presence of 10 $\mu$M retigabine, the current at the holding potential as well as the amplitude of the inward tail currents recorded upon negative potential steps were increased (Fig. 7). In contrast, the amplitude of the outward currents remained almost unchanged. After recording the retigabine-induced effects, application of 100 $\mu$M XE991 totally blocked $I_{Ks}$. Before application of retigabine, 50% of the XE991-sensitive current was activated at $-61.8 \pm 1.0$ mV ($k = 12.4 \pm 1.1$ mV), whereas in the presence of retigabine, 50% of the XE991-sensitive current was already activated at $-85.4 \pm 2.8$ mV ($k = 17.3 \pm 2.5$ mV; mean ± S.E.M.; $n = 4$). This showed that retigabine shifted the activation curve to more negative membrane potentials by −23.6 mV and induced an increase in the slope factor. Retigabine also induced changes in the time course of deactivation and activation. In the presence of retigabine deactivation became slower, the time constant of deactivation of the current elicited with a negative potential step to −130 mV increased by a factor of 2.7 from $\tau = 30.7 \pm 4.0$ ms to $\tau = 83.4 \pm 5.7$ ms (mean ± S.E.M.; $n = 6$), at −110 mV the time constant of deactivation increased by a factor of 2.9 from $58.5 \pm 6.8$ ms (control) to $168.4 \pm 26.5$ ms. In contrast, the time course of activation was accelerated by retigabine; at the holding potential of −70 mV the time constant of current activation following a negative pulse to −130 mV decreased from $\tau = 24.9 \pm 4.8$ ms to $\tau = 4.7 \pm 2.3$ ms (mean ± S.E.M.; $n = 6$).

**Voltage dependence of $I_{Ks}$ activation depends on $[K^+]_o$.** The data described so far showed that 50% of $I_{Ks}$ is activated at about −60 mV if the measurements were made in high $[K^+]_o$. This voltage dependence of $I_{Ks}$ is far more negative than that reported for currents mediated by heterologously expressed KCNQ channels. For KCNQ2 $E_{0.5}$ values of −14 and −18 mV have been reported if CHO cells were used as an expression system (Selyanko *et al.* 2000, 2001) or −37 mV if KCNQ2 channels were expressed in oocytes of *Xenopus laevis* (Biervert *et al.* 1998). Since no data are available about the effect of $[K^+]_o$ on the voltage dependence of $I_{Ks}$ activation, we performed experiments in solutions containing different $K^+$ concentrations (Fig. 8). From a holding potential of −70 mV test pulses of 150 ms duration were followed by a potential step to −100 mV to record tail currents. All experiments were performed in the presence of 1 mM 4-AP to block $K^+$ currents different from $I_{Ks}$ (Dubois, 1981). Figure 8 shows that with increasing $[K^+]_o$ the holding current increased as well as the amplitudes of

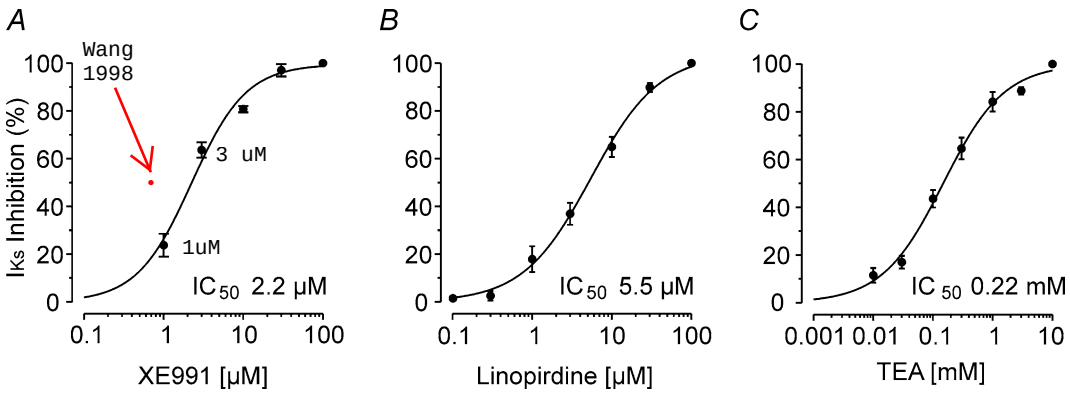


**Figure 6. Dose–response curves of XE991, linopirdine and TEA**
*A*, dose–response curve of XE991. The inhibition of $I_{Ks}$ in the presence of XE991 at concentrations between 1 and 100 $\mu$M was determined from the reduction of the XE991-sensitive tail currents recorded upon repolarization to a holding potential of −75 mV from a 400 ms test pulse to 35 mV. A Hill function was fitted to the data points yielding an $IC_{50} = 2.2$ $\mu$M; Hill coefficient, 1.2; $n = 5$. *B*, dose–response curve of linopirdine. The inhibition of $I_{Ks}$ in the presence of linopirdine at concentrations between 0.1 and 100 $\mu$M was determined from the reduction of the linopirdine-sensitive tail currents recorded upon repolarization to the holding potential of −75 mV from a 400 ms test pulse to 35 mV. A Hill function was fitted to the data points yielding an $IC_{50} = 5.5$ $\mu$M; Hill coefficient, 1.0; $n = 7$. *C*, dose–response curve of TEA. The inhibition of the nodal $K^+$ current was determined from the reduction of the tail currents recorded upon repolarization to the holding potential of −75 mV from a 400 ms test pulse to 35 mV. The effect of 10 mM TEA was assumed to be maximal. The membrane current recorded in the presence of 10 mM TEA was subtracted from the tail currents recorded at lower TEA concentrations. The difference currents were normalized to the control tail current amplitude recorded in the absence of TEA. The means ± S.E.M. were plotted against the TEA concentration. A Hill function was fitted to the data points yielding an $IC_{50} = 0.22$ mM; Hill coefficient, 0.75; $n = 5$.

the tail currents. The tail currents recorded in isotonic KCl were totally blocked by linopirdine (Fig. 8*Af*). This result allowed us to determine the activation curves from the tail current amplitudes. The main result of this and three other experiments was that upon increasing $[K^+]_o$ the activation curves shifted to more negative membrane potentials and their slope factors decreased. Mean values ($\pm$ S.E.M.; $n = 4$) of $E_{0.5}$ and slope factors of the activation curves were: $E_{0.5} = -40.5 \pm 2.8$ mV, $k = 21.7 \pm 1.3$ mV (10 mM KCl); $E_{0.5} = -57.0 \pm 2.6$ mV, $k = 15.9 \pm 2.0$ mV (80 mM KCl); $E_{0.5} = -64.4 \pm 2.4$ mV, $k = 15.8 \pm 1.4$ mV (160 mM KCl). $E_{0.5}$ shifted by about 25 mV upon a change from 10 mM to 160 mM $[K^+]_o$. Figure 8*Aa* shows that the tail current amplitudes recorded in Ringer solution were small. In other fibres we found that these small tail currents were totally blocked by XE991 or linopirdine. A tentative evaluation of these tail currents recorded in Ringer solution showed that 50% of $I_{Ks}$ was activated near $-25$ mV and that the slope of the activation curve was flatter than that in 10 mM KCl. The activation curve obtained from the data in Fig. 8*Aa* was included in the graph of Fig. 8*B*, but different symbols were used to indicate that these results are less certain, on account of the small amplitude of the currents. Nevertheless these data indicated that in Ringer solution part of $I_{Ks}$ is already activated at the normal resting potential of these fibres and that activation of $I_{Ks}$ and that of heterologously expressed KCNQ2 currents takes place within a similar potential range.

**Action potentials.** Since the time course of $I_{Ks}$ activation is slow, it barely influences the shape of an action potential (Reid *et al.* 1993). In contrast, it has been assumed that $I_{Ks}$ plays an important role in accommodation to subthreshold depolarizing current, in spike-frequency adaptation and in stabilizing the resting membrane potential (Dubois, 1981; Baker *et al.* 1987; Reid *et al.* 1993; Schwarz *et al.* 1995). In the past, these presumed functions of $I_{Ks}$ in the node of Ranvier could not be tested directly, because a selective inhibitor of $I_{Ks}$ was not available. Since the voltage-clamp experiments described above show that XE991 selectively blocks $I_{Ks}$, we used this substance to investigate the function of $I_{Ks}$ in current-clamp experiments. Figure 9*A* shows that 100 $\mu$M XE991 neither influenced the amplitude nor the duration of action potentials elicited with short depolarizing currents. In five fibres the action potential amplitude was $109.6 \pm 2.5$ mV (mean $\pm$ S.E.M.) and its duration near the threshold potential was $1.25 \pm 0.07$ ms in Ringer solution. In the presence of 100 $\mu$M XE991

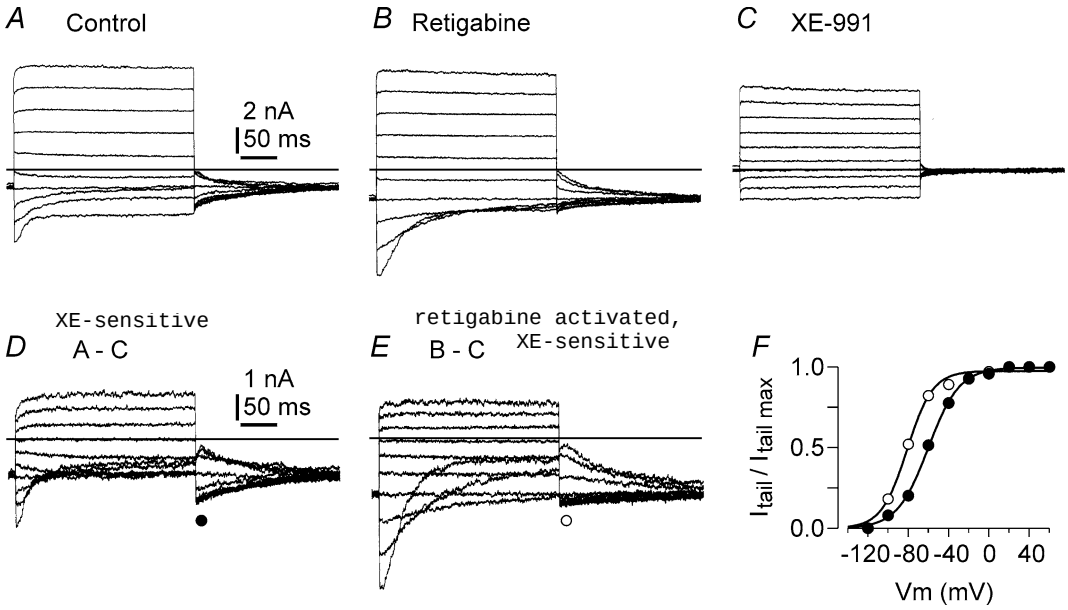


**Figure 7. Retigabine activates $I_{Ks}$**
*A* and *B*, membrane currents recorded in isotonic KCl. Holding potential, $-60$ mV. Hyperpolarizing and depolarizing pulses were applied in steps of 20 mV in the absence (*A*, Control) and presence of retigabine (10 $\mu$M; *B*). *C*, membrane currents recorded after application of XE991 (100 $\mu$M). *D*, XE991-sensitive current obtained by subtracting the membrane current traces shown in *C* from those in *A*. *E*, XE991-sensitive currents in the presence of retigabine obtained by subtracting the membrane currents shown in *C* from those in *B*. *F*, activation curves, determined from the amplitudes of the tail currents recorded upon repolarization to the holding potential shown in *D* (Control) and *E* (XE991-sensitive current in the presence of retigabine). The tail current amplitudes were normalized and plotted against test potentials. Boltzmann functions were fitted to the data points yielding $V_{0.5} = -61$ mV (slope factor = 15.8 mV) for the XE991-sensitive current (Control) and $V_{0.5} = -85.6$ mV (slope factor = 15.5 mV) for the activation curve of the XE991-sensitive current in the presence of retigabine.

these values did not change significantly; the action potential amplitude was 110.0 ± 2.3 mV and its duration near the threshold potential 1.28 ± 0.10 ms. Nevertheless, application of XE991 induced a small depolarization of the resting membrane potential (4.2 ± 2.0 mV) and slightly decreased the threshold potential for eliciting an action potential, from 22.6 ± 0.9 to 19.0 ± 1.8 mV. Figure 8*B* shows current-clamp recordings in a nerve fibre which responded with repetitive activity to a long lasting depolarizing current stimulus in normal Ringer solution. In the control (Fig. 8*Ba*), the amplitude of the stimulating current was adjusted to elicit just one action potential. In the presence of XE991, the same depolarizing current amplitude elicited three successive action potentials (Fig. 9*Bb*). A similar observation was made in one other nerve fibre which exhibited repetitive activity before application of the drugs. The other three fibres investigated did not exhibit repetitive activity. In the rat, motor as well as sensory nerve fibres are able to fire repetitively, therefore this property cannot be used to distinguish between the two fibre types (reviewed by Vogel & Schwarz, 1995).

The effects of XE991 on threshold potential and frequency adaptation in the isolated rat nerve fibre were rather small compared with the drastic effects of XE991 in the *in vivo* experiments described below. This is most likely caused by the unspecific damage of the nerve fibres during the dissection procedure. We therefore studied the function of $I_{Ks}$ on the excitability properties of peripheral motor nerve fibres in experiments performed *in vivo* in which the damage of nerve fibres due to mechanical manipulation was avoided.

### *In vivo* experiments

**Threshold electrotonus.** Bostock & Baker (1988) showed that it is possible to detect the effects of $I_{Ks}$ on the response of axons to subthreshold polarizing currents (i.e. electrotonus) by threshold tracking (i.e. threshold electrotonus) and that this method can be applied *in vivo*. The accommodative sag in the response to depolarizing currents was prevented *in vitro* by TEA and attributed to increased activation of $I_{Ks}$ (Bostock & Baker, 1988). Figure 10 illustrates the effects of XE991 on this manifestation of $I_{Ks}$ *in vivo*. Figure 10*A* shows a family of threshold electrotonus curves for motor axons in the tail of a rat, for 100 ms currents set to ±20 and ±40% of resting threshold. There is a rapid phase of threshold

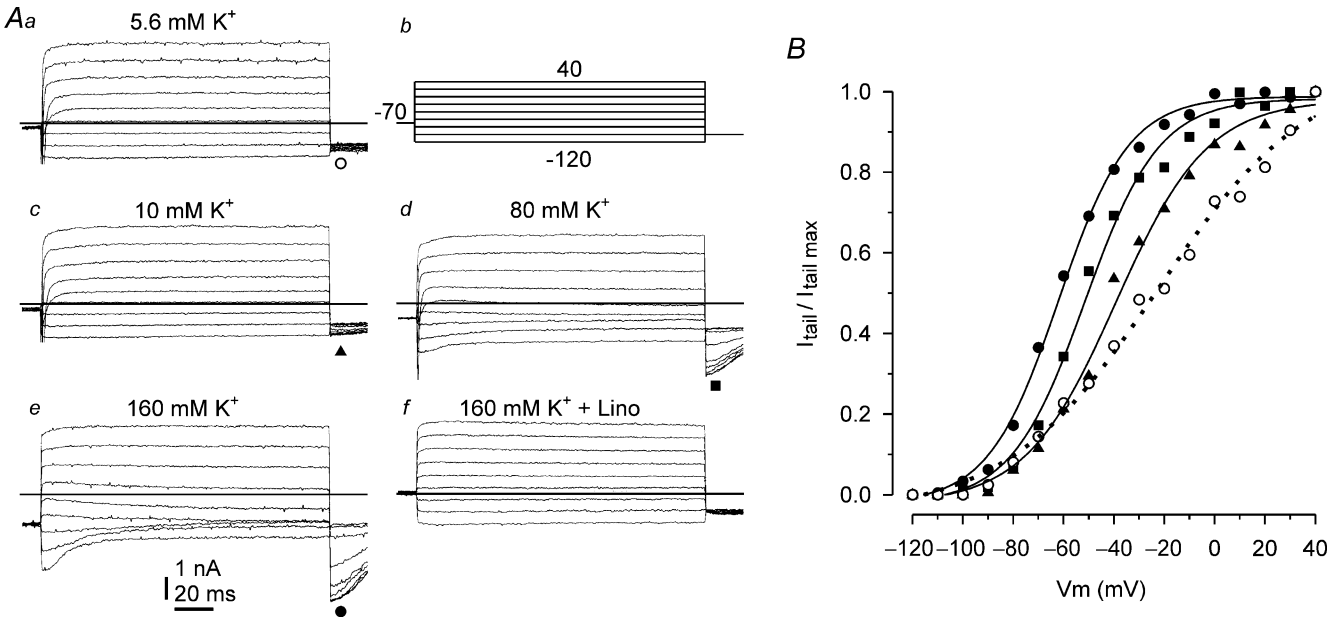


**Figure 8. $I_{Ks}$ activation curve is shifted to more negative membrane potentials upon increasing $[K^+]_o$**
*Aa,* and *c–e*, membrane currents recorded in Ringer solution (5.6 mM), and in solutions with increasing $[K^+]_o$ (10, 80 and 160 mM $K^+$). *Af*, family of membrane currents recorded in 160 mM KCl containing 100 μM linopirdine. *Ab*, pulse protocol. Holding potential, −70 mV. $Na^+$ inward currents were cut off. *B*, activation curves. Normalized tail current amplitudes of the currents shown in panels *Aa–e* were plotted against test pulse potentials. Boltzmann functions were fitted to the data points. Values for 50% activation ($E_{0.5}$) and the slope factor *k*: Ringer (○; $E_{0.5} = -22.8$ mV; $k = 30.2$ mV); 10 mM KCl (▲; $E_{0.5} = -39.1$ mV; $k = 18.1$ mV); 80 mM KCl (■; $E_{0.5} = -51.4$ mV; $k = 14.7$ mV); isotonic KCL (●; $E_{0.5} = -61.9$ mV; $k = 14.0$ mV).

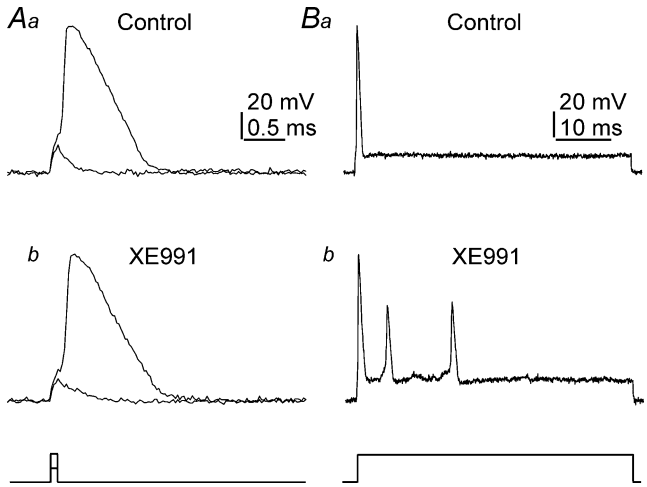


**Figure 9. XE991 reduces threshold potential**
*A*, local responses and action potentials elicited with 0.1 ms depolarizing sub- and suprathreshold currents, respectively, in the absence (*Aa*, control) and presence of XE991 (100 $\mu$M; *Ab*), recorded from a node of Ranvier of a single myelinated nerve fibre. *B*, action potentials recorded with 45 ms depolarizing pulses in normal Ringer solution (*Ba*), and in Ringer solution containing 100 $\mu$M XE991 (*Bb*). All nerve fibre responses were elicited with the same depolarizing current amplitude from a single myelinated nerve fibre.

change at current onset and offset, due to the change in nodal membrane potential, followed by slower changes due to the change in potential of the internodal axolemma (most pronounced with the 40% hyperpolarizing current) and the activation or deactivation of slow $K^+$ currents (most pronounced with the 40% depolarizing current). These recordings resemble those in humans (e.g. Kiernan *et al.* 2000), although the accommodative sag in the responses to the depolarizing currents is less pronounced in the rat. After injection of XE991 (2.5 mg kg$^{-1}$ I.P.) the accommodative sag to depolarizing currents was abolished altogether (Fig. 10*B*). This effect was highly repeatable, and Fig. 10*C* shows the mean ± S.E.M. of the waveforms obtained from five such experiments (40% depolarizing current only). XE991 abolished both the slow accommodation to the depolarization and the post-depolarization undershoot in threshold reduction, which has also been used as a measure of $I_{Ks}$ (e.g. Kiernan *et al.* 2001). Since $I_{Ks}$ is already partly activated at the resting potential, there is also a small effect on the responses to hyperpolarizing currents, and abolition of the post-hyperpolarization (or 'anode break') increase in excitability (Fig. 10*A* and *B*).

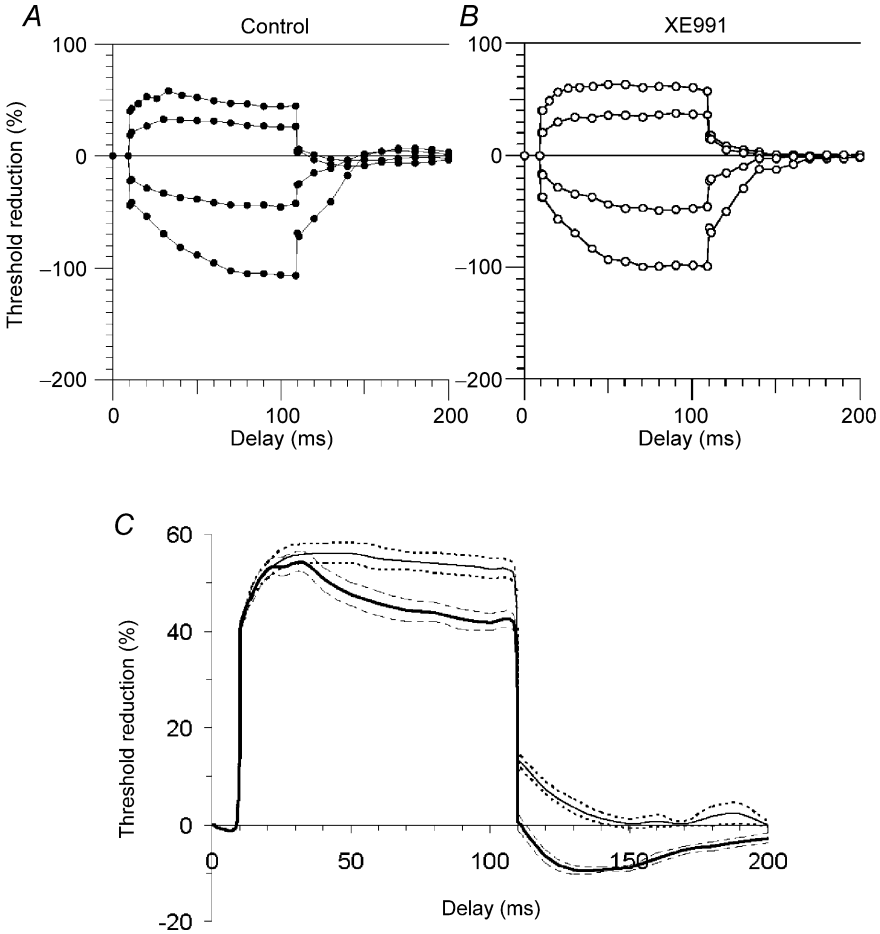


**Figure 10. Effects of XE991 on threshold electrotonus**
*A*, threshold changes produced in motor axons innervating the tail muscles of an anaesthetized rat by 100 ms rectangular current pulses set to ±20 and ±40% of control threshold. Threshold reduction, or increase in excitability, plotted upwards. *B*, threshold electrotonus recorded as in *A* after injection of XE991 (2.5 mg kg$^{-1}$ I.P.). *C*, mean ± S.E.M. of 5 such recordings (+40% of control threshold) from different rats, showing excellent repeatability of these excitability changes (thick continuous line, control, thin line, post-XE991).

**Recovery cycles for one and seven conditioning stimuli.** The filled circles in Fig. 11*Aa* show the recovery cycle for motor axons in the tail of a rat after a single supramaximal stimulus. The excitability changes qualitatively resemble those in human median nerve axons (Kiernan *et al.* 2000), with successive phases of relative refractoriness (up to 3 ms), superexcitability (between 3 and about 30 ms) and late subexcitability (between 30 and 200 ms). However,

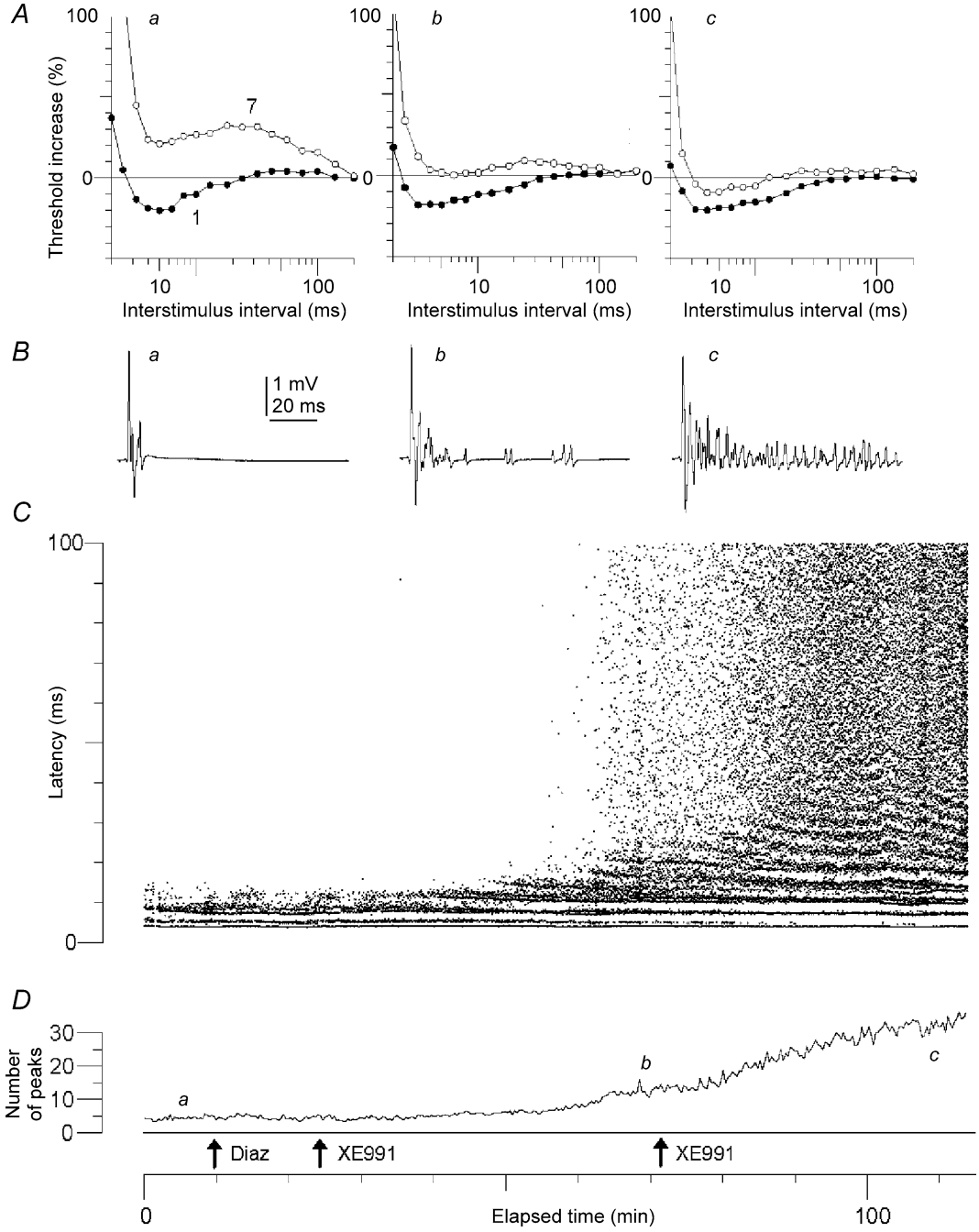


**Figure 11. Effects of XE991 on recovery cycles and spike-frequency adaptation**
*A*, recovery cycles recorded with 1 (●) and 7 (○) supramaximal conditioning stimuli in rat tail motor axons. Multiple conditioning stimuli at short (4 ms) intervals enhance the long-lasting subexcitability, due primarily to increased activation of $I_{Ks}$. The letters *a, b* and *c* refer to recordings made at the times shown in *D*, i.e. control, post-1.25 mg kg$^{-1}$ XE991 and post-2.5 mg kg$^{-1}$ XE991. *B*, electromyograms recorded from rat tail muscles to 100 ms suprathreshold rectangular current pulses at the times indicated in *D*. *C*, raster plot of latencies of all peaks in the electromyograms for responses to the 100 ms current pulses as in *B* plotted against elapsed time (axis as in *D*). *D*, numbers of peaks in the responses to 100 ms current pulses as in *B* and *C*. Letters indicate times of recordings in *A* and *B*. Arrows indicate times of I.P. drug injections: Diaz, 2 mg kg$^{-1}$ diazepam; XE991, 1.25 mg kg$^{-1}$ XE991.

the late subexcitability, attributed to $I_{Ks}$, is considerably smaller in the rat. To amplify this manifestation of $I_{Ks}$, we substituted a train of seven conditioning stimuli at 250 Hz (open circles in Fig. 11*Aa*). Bergmans (1970) used a similar protocol to enhance the subexcitability, which he called $H_1$ (i.e. first hyperpolarizing afterpotential), to distinguish it from $H_2$, the second hyperpolarizing afterpotential due to activation of the $Na^+$ pump by long trains of impulses. The change in the recovery cycle with the number of conditioning impulses in Fig. 11*Aa* is qualitatively similar to that seen in human median motor axons (Fig. 22 in Bergmans, 1970). After injection of XE991, the late subexcitability, and the difference between the effects of one and seven conditioning stimuli largely disappeared, indicating that KCNQ channels are also responsible for these manifestations of $I_{Ks}$ (Fig. 11*Ab* and *c*).

**Spike frequency adaptation.** In response to a prolonged suprathreshold stimulus, axons may produce a train of impulses, but there is a progressive reduction in impulse frequency, usually leading to cessation of repetitive activity. This spike-frequency adaptation is particularly pronounced in motor fibres, which normally produce two or at most three impulses, however strong the depolarizing current (Bostock, 1995). In rat motor fibres the adaptation is reduced by TEA, and has been related to the subthreshold accommodation and also attributed to activation of $I_{Ks}$, which increases in a stepwise fashion with successive nerve impulses (Baker *et al.* 1987; Schwarz *et al.* 1995). We tested for a contribution of KCNQ channels to spike-frequency adaptation *in vivo*, by alternating the tests of excitability with a suprathreshold 100 ms stimulus, equal in amplitude to the 1 ms test stimulus that produced a compound muscle action potential (CMAP) that was 40% of maximal. Figure 11*B–D* illustrates the result of one such experiment. Initially spike-frequency adaptation was pronounced, and there were usually only two peaks in the electromyogram (Fig. 11*Ba*), indicating that a significant proportion of fibres were firing twice, but triple discharges were rare. Injection of diazepam ($2\,mg\,kg^{-1}$) had no discernible effect (Fig. 11*C* and *Da*). However, XE991 ($1.25\,mg\,kg^{-1}$) produced a slow build-up of repetitive activity, which appeared to reach a plateau after about 45 min (Fig. 11*Bb* and *Db*), but after a second injection of XE991 ($1.25\,mg\,kg^{-1}$) increased still further. Similar inhibition of spike-frequency adaptation was seen in two further experiments with long suprathreshold current pulses. It is clear that KCNQ channels make a major contribution to spike-frequency adaptation in these rat motor axons.

## Discussion

Our immunostaining results show that KCNQ2 channel proteins are present in all nodes of Ranvier in peripheral myelinated nerve fibres, whereas strong labelling for KCNQ3 channel proteins was likely to be found in nodes of small and medium sized nerve fibres, but was absent in large myelinated nerve fibres. The slowly activating $K^+$ current ($I_{Ks}$) recorded in large myelinated nerve fibres was totally inhibited by the selective KCNQ channel blockers XE991 and linopirdine, and it was activated by retigabine, a selective KCNQ channel opener. Voltage-dependent activation of $I_{Ks}$ was shown to be dependent on extracellular $[K^+]$. *In vivo,* XE991 induced a drastic reduction of both subthreshold accommodation (as measured by threshold electrotonus) and spike-frequency adaptation to suprathreshold depolarizing currents. Taken together, these immunocytochemical, biophysical and pharmacological data strongly indicate that $I_{Ks}$ is mediated by KCNQ channels, and provide new evidence that $I_{Ks}$ serves to stabilize the nodal membrane potential. Furthermore, $I_{Ks}$ in the large rat sciatic nerve fibres studied here appears to be mediated by homomeric KCNQ2 channels.

### Indications that $I_{Ks}$ is mediated by KCNQ channels

The pharmacological experiments we performed provide compelling evidence that $I_{Ks}$ is mediated by KCNQ channels. Linopirdine and XE991 are selective KCNQ channel blockers (Lamas *et al.* 1997; Wang *et al.* 1998) that inhibit $I_{Ks}$, $I_M$ and heterologously expressed KCNQ currents with similar potency. Thus, XE991 blocks $I_{Ks}$ with an $IC_{50}$ ($2.2\,\mu M$) only slightly higher than that reported by Wang *et al.* (1998) for blocking currents mediated by heterologously expressed KCNQ2 ($0.71\,\mu M$), KCNQ2/3 ($0.6\,\mu M$) and M-channels in sympathetic neurons ($0.98\,\mu M$). Linopirdine blocks $I_{Ks}$ with an $IC_{50}$ ($5.5\,\mu M$) very similar to the values reported for blockage of KCNQ2 ($4.8\,\mu M$), KCNQ3 ($4.8\,\mu M$), KCNQ2/3 ($4.0\,\mu M$) and M-channels ($7.0\,\mu M$; Hadley *et al.* 2000; Wang *et al.* 1998).

Although KCNQ2 and KCNQ3 are similar in their sensitivity to XE991 and linopirdine, they have a very different sensitivity to TEA. The higher sensitivity of KCNQ2 to TEA results from the presence of a single pore tyrosine residue located just downstream of the canonical GYG sequence (Hadley *et al.* 2000). In *Xenopus laevis* oocytes, KCNQ2 homomers and KCNQ2/3 heteromers exhibit TEA $IC_{50}$ values of 0.16 and 3.5 mM, respectively (Wang *et al.* 1998). Values obtained in CHO cells are similar (KCNQ2: $IC_{50} = 0.3$ mM; KCNQ2/3: 3.8 mM; Hadley *et al.* 2000). KCNQ3 homomeric channels are very insensitive to TEA, with even high TEA concentrations ($> 30$ mM) showing only minimal effects (Hadley *et al.* 2000). The $IC_{50}$ for TEA block of $I_{Ks}$ (0.22 mM) found in the present experiments is nearly the same as for homomeric KCNQ2 channels; this $IC_{50}$ is at least 15-fold less for KCNQ2/3 channels or native M-currents (Wang *et al.* 1998;

Hadley *et al.* 2000). Data for TEA inhibition of $I_{Ks}$ was well fitted assuming a single homogeneous population of binding sites. These results are unlike those obtained in neurons from dorsal root ganglion (Passmore *et al.* 2003) and neurons of the superior sympathetic ganglion of immature animals (Hadley *et al.* 2003), where data suggest that a mixture of KCNQ2 and KCNQ2/3 channels are expressed.

$I_{Ks}$ is also activated by the selective KCNQ channel opener retigabine (Rundfeldt, 1997; Rundfeldt & Netzer, 2000; Wickenden *et al.* 2000; Tatulian *et al.* 2001). Retigabine (10 $\mu$M) shifts the $I_{Ks}$ activation curve to more negative membrane potentials by −24 mV. This shift is the same as the shift in KCNQ2 currents (−24 mV), but less than shifts measured for KCNQ3 (−43 mV) and KCNQ2/3 (−30 mV) currents (Tatulian *et al.* 2001). In addition, retigabine accelerates activation and slows deactivation kinetics of $I_{Ks}$, changes which have also been reported in KCNQ-mediated currents (Wickenden *et al.* 2000).

In addition to these pharmacological properties, we discovered a novel and, potentially, physiologically significant shared property of KCNQ2 channels and $I_{Ks}$, the sensitivity of voltage-dependent activation to extracellular $[K^+]$. Owing to the small size of $I_{Ks}$ and its gating in the voltage range near physiological $E_K$, previous recordings at both macroscopic and single channel levels have been performed in the presence of elevated extracellular $[K^+]$. The new availability of the selective $I_{Ks}$ blocking substances, XE991 and linopirdine, prompted us to study $I_{Ks}$ also at lower concentrations of extracellular $[K^+]$. We found that the voltage dependence of $I_{Ks}$ activation is very sensitive to $[K^+]_o$. In addition to a shift to more positive potentials, the activation curves become flatter upon decreasing $[K^+]_o$, suggesting that part of $I_{Ks}$ is already activated at the normal resting potential, despite the shift to more positive membrane potentials. We are not aware of any previous studies investigating the dependence of the biophysical properties of KCNQ channels or of the M-current on $[K^+]_o$. The cellular or molecular mechanisms underlying the large shift of the activation curve to more negative membrane potentials by 30–40 mV upon changing the external $K^+$ concentration from 5.6 mM in Ringer to isotonic KCl solution are unknown. Previous voltage-clamp measurements of the nodal $I_{Ks}$ in frog (Dubois, 1981) and rat nerve fibres (Röper & Schwarz, 1989) were performed in isotonic KCl and yielded activation curves with 50% activation at −60 mV. A similar voltage dependence of the activation curve of nodal S channels presumably mediating $I_{Ks}$ was derived from single channel recordings in isotonic KCl solution by using the patch-clamp method in demyelinated nerve fibres. These studies show that 50% of the S channels are activated at −76 mV in rat (Safronov *et al.* 1993) and at −68 mV in human nerve fibres (Reid *et al.* 1999). Preliminary experiments in CHO cells expressing KCNQ2 channels have shown that the voltage dependence of activation of the KCNQ2-mediated current was shifted by about 20 mV to more negative membrane potentials upon a change from Ringer to isotonic KCl solution (G. Glassmeier & JR Schwarz, unpublished data). Further experiments have to be done to explain the high sensitivity of $I_{Ks}$ activation to $[K^+]_o$. Regardless of the underlying mechanism, this novel feature further supports the idea that KCNQ subunits (KCNQ2 by other criteria noted above) mediate $I_{Ks}$.

In summary, our nodal recordings strongly suggest that, in the largest fibres of sciatic nerve of the rat, $I_{Ks}$ is mediated by homomeric KCNQ2 channels. The immunocytochemistry also supports this, but conclusions drawn from this approach alone were limited by the current lack of antibodies against the alternatively spliced KCNQ3 isoform, i.e. KCNQ3a. Since KCNQ3a is quite TEA insensitive (Wang *et al.* 1998), it is unlikely that this subunit makes a significant contribution to $I_{Ks}$ in these large fibres.

Of native neuronal currents so far attributed to KCNQ subunits, $I_{Ks}$ is the first current apparently mediated exclusively by homomeric KCNQ2 channels. The somatic M-current of sympathetic and dorsal root ganglia, hippocampus, and striatal medium spiny neurons are all primarily mediated by heteromeric KCNQ2/3 channels (Wang *et al.* 1998; Passmore *et al.* 2003; Hadley *et al.* 2003; Shen *et al.* 2005). $I_{Ks}$ activation and deactivation kinetics are considerably faster than those of KCNQ currents or native neuronal M-currents. We cannot explain these differences, although interaction with as yet unidentified proteins in the node or post-translational modifications are potential mechanisms. The basis for this must be explored in future work.

### Distinctive distribution of ion channels in the node of Ranvier

Mammalian nodes of Ranvier exhibit a complex distribution of ion channels: $Na_v1.6$ channels are located at a very high density in the nodal axolemma, whereas the delayed rectifier $K^+$ channels $K_v1.1$ and $K_v1.2$ are predominantly confined to the juxtaparanodes (reviewed in Vogel & Schwarz, 1995; Poliak & Peles, 2003; Scherer *et al.* 2004). Devaux *et al.* (2004) showed that KCNQ2 channel proteins are present in the node of Ranvier and that they are co-localized with $Na^+$ channel proteins and not with the juxtaparanodal Kv1.1 and Kv1.2 channels. These findings nicely correspond to the previous electrophysiological finding that the nodal $I_{Ks}$ density is about 30 times larger than the internodal $I_{Ks}$ (Röper & Schwarz, 1989). KCNQ3 channel proteins are also present in peripheral nerve fibres, but they seem to be located predominantly in the myelin; staining of KCNQ3 proteins in the nodal axolemma of peripheral nerve fibres was scarcely detected (Devaux *et al.* 2004). Our present data

extend these previous results. In addition, we observed a more wide-spread staining of nodes for KCNQ3. While strong nodal staining for the KCNQ3 channel protein was found in up to 50% of small and medium-sized nerve fibres, such strong KCNQ3 staining was absent in nodes of large-diameter fibres. Since only the largest fibres were dissected for voltage-clamp experiments, the $I_{Ks}$ data presented in this paper were obtained from nodes of Ranvier presumably containing only KCNQ2 channels. Since an antibody against the alternatively spliced form of KCNQ3 is not available, we could not exclude the possibility that this isoform was also present in nodal membranes by immunohistochemistry. The co-localization of KCNQ2 and KCNQ3 channels in the nodes of Ranvier in about 50% of the sampled small and medium-sized nerve fibres suggests that heteromeric KCNQ2/3 channels may exist in these fibres. However, at present there are no data available about the properties and function of $I_{Ks}$ in these fibres with smaller diameters. We also do not know whether the nerve fibres which contain nodal KCNQ3 channels are correlated with a certain function. One possibility could be that some types of sensory nerve fibres are equipped with a different set of ion channels than motor nerve fibres. Although in amphibian nerve sensory and motor axons can be distinguished by differences in their biophysical properties (summarized in Vogel & Schwarz, 1995), these differences are more subtle in mammalian nerve fibres. Compared with sensory fibres, motor fibres probably express a smaller persistent $Na^+$ conductance (Bostock & Rothwell, 1997) and less inward rectification mediated by the hyperpolarization-activated $I_h$ (Bostock *et al.* 1994), but these differences are too small to be detected in recordings of macroscopic currents measured with the Nonner clamp method used in the present experiments.

### Function of $I_{Ks}$

Since the voltage dependence of $I_{Ks}$ activation in normal extracellular $[K^+]$ is relatively shallow, a small proportion of channels is expected to be activated at the resting potential. This explains how inhibition of $I_{Ks}$ by XE991 induced a depolarization of a few millivolts and a slight reduction in the threshold potential in our experiments. Because of its slow activation kinetics and its small amplitude, $I_{Ks}$ may exert little influence on repolarization of the action potential, and, consistent with this, we did not observe a significant change in the shape of the action potential after application of XE991. Due to the slow time course of deactivation, the amplitude of $I_{Ks}$ successively increases during repetitive activity since part of $I_{Ks}$ is activated by each action potential (Reid *et al.* 1993). This accumulation of $I_{Ks}$ induces frequency adaptation. Since repetitive action potential firing may lead to a local increase in the $K^+$ concentration in the nodal gap, this may shift the activation curve to more negative membrane potentials, thereby effectively increasing the amplitude of activated $I_{Ks}$. In our current-clamp experiments, total inhibition of $I_{Ks}$ by XE991 decreased frequency adaptation and in the *in vivo* experiments it was virtually abolished. This accommodative function of $I_{Ks}$ was first proposed by Dubois (1981, 1983). Later, the stabilizing function on membrane excitability and its role for frequency adaptation were clearly demonstrated experimentally in rat ventral root fibres by application of TEA (Baker *et al.* 1987). However, the present study is the first to demonstrate the function of $I_{Ks}$ by using a selective KCNQ blocker as a pharmacological tool. Patients with a point mutation in the S4 domain of KCNQ2 (R207W) suffer from myokymia and exhibit a loss of frequency adaptation (Dedek *et al.* 2001) very similar to that observed in the anaesthetized rat after pharmacological blockage of $I_{Ks}$.

The separate contributions of fast and slow $K^+$ channels to the electrical properties of myelinated axons were shown by studies of electrotonus and afterpotentials in rat spinal roots (Baker *et al.* 1987), using 4-aminopyridine and TEA, respectively, as selective channel blockers. After the inital fast change in potential (F component) on applying a 100 ms depolarizing current, there was a further slow depolarization (S1 component), attributed to depolarization of the internodal axolemma, followed by a slow repolarization (S2 component), that was blocked by TEA and attributed to $I_{Ks}$. Similar components can be seen in the accompanying changes in threshold (i.e. threshold electrotonus), where the S2 component appears as an accommodative increase in threshold. Excitability testing therefore enables these $K^+$ channel functions to be investigated *in vivo* (Bostock & Baker, 1988; Yang *et al.* 2000). In our experiments I.P. injection of XE991 abolished all nerve fibre excitability functions attributed to $I_{Ks}$, i.e. accommodation to 100 ms subthreshold depolarizing currents as well as the post-depolarization undershoot in excitability. In addition, the late subexcitability after a single impulse or a short train of seven impulses was totally inhibited by XE991.

The *in vivo* experiments clearly show that blockage of $I_{Ks}$ induces a drastic increase in the excitability of motor nerve fibres. Such a degree of hyperexcitability was only obtained in current-clamp experiments done on single nerve fibres isolated from the sciatic nerve under extreme artificial conditions, such as a total blockage of $K^+$ currents by TEA in addition to full removal of external $Ca^{2+}$ (Bergmann *et al.* 1968). The nerve fibres isolated from the sciatic nerve for voltage clamping may have been damaged during the dissection procedure, thereby increasing, for example, the unspecific leakage current. This could explain why these nerve fibres did not exhibit such a degree of repetitive activity as in the *in vivo* experiments testing the recovery cycle. These observations are in line with the finding that a mutation (R207W) in the voltage sensor of KCNQ2 channels causes myokymia and neonatal epilepsy (see above; Dedek *et al.* 2001).

In conclusion, we have shown beyond reasonable doubt that the slow potassium current at rat nodes of Ranvier, designated $I_{Ks}$, is generated by XE991-sensitive KCNQ channels. In the largest fibres, these channels appear to be KCNQ2 homomers. This has been shown at the level of the membrane currents in isolated nodes of Ranvier by their distinct pharmacology, and the *in vivo* recordings have confirmed that all the nerve excitability functions previously attributed to $I_{Ks}$, such as accommodation, spike-frequency adaptation and late subexcitability in the recovery cycle, are indeed caused by this current and generated by KCNQ channels. The functional contribution of the KCNQ3 subunits detected at nodes of smaller diameter fibres, and in myelin sheaths, remains obscure.

## References


Baker M & Bostock H (1989). Depolarization changes the mechanism of accommodation in rat and human motor axons. *J Physiol* **411**, 545–561.

Baker M, Bostock H, Grafe P & Martius P (1987). Function and distribution of three types of rectifying channel in rat spinal root myelinated axons. *J Physiol* **383**, 45–67.

Bergmann C, Nonner W & Stämpfli R (1968). Sustained spontaneous activity of Ranvier nodes induced by the combined action of TEA and lack of calcium. *Pflugers Arch* **302**, 24–37.

Bergmans J (1970). *The Physiology of Single Human Nerve Fibres*. University of Louvain, Vander, Belgium.

Biervert C, Schroeder BC, Kubisch C, Berkovic SF, Propping P, Jentsch TJ & Steinlein OK (1998). A potassium channel mutation in neonatal human epilepsy. *Science* **279**, 403–406.

Bostock H (1995). Mechanisms of accommodation and adaptation in myelinated axons. In *The Axon*, ed. Waxman SG, Stys PK & Kocsis JD, pp. 311–327. Oxford University Press, Oxford.

Bostock H & Baker M (1988). Evidence for two types of potassium channel in human motor axons in vivo. *Brain Res* **462**, 354–358.

Bostock H, Burke D & Hales JP (1994). Differences in behaviour of sensory and motor axons following release of ischaemia. *Brain* **117**, 225–234.

Bostock H, Cikurel K & Burke D (1998). Threshold tracking techniques in the study of human peripheral nerve. *Muscle Nerve* **21**, 137–158.

Bostock H & Rothwell JC (1997). Latent addition in motor and sensory fibres of human peripheral nerve. *J Physiol* **498**, 277–294.

Brismar T (1980). Potential clamp analysis of membrane currents in rat myelinated nerve fibres. *J Physiol* **298**, 171–184.

Brown DA (1988). M currents. In *Ion Channels 1*, ed. Narahashi T, pp. 55–94. Plenum Press, New York & London.

Burke D, Kiernan MC & Bostock H (2001). Excitability of human axons. *Clin Neurophysiol* **112**, 1575–1585.

Cooper EC, Harrington E, Jan YN & Jan LY (2001). M channel KCNQ2 subunits are localized to key sites for control of neuronal network oscillations and synchronization in mouse brain. *J Neurosci* **21**, 9529–9540.

Dedek K, Kunath B, Kananura C, Reuner U, Jentsch TJ & Steinlein OK (2001). Myokymia and neonatal epilepsy caused by a mutation in the voltage sensor of the KCNQ2 $K^+$ channel. *PNAS* **98**, 12272–12277.

Delmas P & Brown DA (2005). Pathways modulating neural KCNQ/M (Kv7) potassium channels. *Nat Rev Neurosci* **6**, 850–862.

Devaux JJ, Kleopa KA, Cooper EC & Scherer SS (2004). KCNQ2 is a nodal $K^+$ channel. *J Neurosci* **24**, 1236–1244.

Dubois JM (1981). Evidence for the existence of three types of potassium channels in the frog Ranvier node membrane. *J Physiol* **318**, 297–316.

Dubois JM (1983). Potassium currents in the frog node of Ranvier. *Prog Biophys Mol Biol* **42**, 1–20.

Gokin AP, Philip B & Strichartz GR (2001). Preferential block of small myelinated sensory and motor fibres by lidocaine: in vivo electrophysiology in the rat sciatic nerve. *Anesthesiology* **95**, 1441–1454.

Hadley JK, Noda M, Selyanko AA, Wood IC, Abogadie FC & Brown DA (2000). Differential tetraethylammonium sensitivity of KCNQ1-4 potassium channels. *Br J Pharmacol* **129**, 413–415.

Hadley JK, Passmore GM, Tatulian L, Al-Qatari M, Ye F, Wickenden AD & Brown DA (2003). Stoichiometry of expressed KCNQ2/KCNQ3 potassium channels and subunit composition of native ganglionic M channels deduced from block by tetraethylammonium. *J Neurosci* **23**, 5012–5019.

Jentsch TJ (2000). Neuronal KCNQ potassium channels: physiology and disease. *Nature Rev Neurosci* **1**, 21–30.

Kiernan MC, Burke D, Andersen KV & Bostock H (2000). Multiple measures of axonal excitability: a new approach in clinical testing. *Muscle Nerve* **23**, 399–409.

Kiernan MC, Hart IK & Bostock H (2001). Excitability properties of motor axons in patients with spontaneous motor unit activity. *J Neurol Neurosurg Psychiatry* **70**, 56–64.

Lamas JA, Selyanko AA & Brown DA (1997). Effects of a cognition enhancer, Linopirdine (DuP 996), on M-type potassium currents ($I_K$(M)) and some other voltage- and ligand-gated membrane currents in rat sympathetic neurons. *Europ J Neurosci* **9**, 605–616.

Neumcke B, Schwarz JR & Stämpfli R (1987). A comparison of sodium currents in rat and frog myelinated nerve: normal and modified sodium inactivation. *J Physiol* **382**, 175–191.

Neumcke B & Stämpfli R (1982). Sodium currents and sodium-current fluctuations in rat myelinated nerve fibres. *J Physiol* **329**, 163–184.

Nonner W (1969). A new voltage clamp method for Ranvier nodes. *Pflugers Arch* **309**, 176–192.

Pan Z, Selyanko AA, Hadley JK, Brown DA, Dixon JE & McKinnon D (2001). Alternative splicing of KCNQ2 potassium channel transcripts contributes to the functional diversity of M-currents. *J Physiol* **531**, 347–358.

Passmore GM, Selyanko AA, Mistry M, Al-Qatari M, Marsh SS, Matthews EA, Dickenson AH, Brown TA, Burbidge SA, Main M & Brown DA (2003). KCNQ/M currents in sensory neurons: significance for pain therapy. *J Neurosc* **23**, 7227–7236.

Poliak S & Peles E (2003). The local differentiation of myelinated axons at nodes of Ranvier. *Nature Rev Neurosci* **4**, 968–980.

Rasband MN, Trimmer JS, Schwarz TL, Levinson SR, Ellisman MH, Schachner M & Shrager P (1998). Potassium channel distribution, clustering, and function in remyelinating rat axons. *J Neurosci* **18**, 36–47.

Reid G, Bostock H & Schwarz JR (1993). Quantitative description of action potentials and membrane currents in human node of Ranvier. *J Physiol* **467**, 247*P*.

Reid G, Scholz A, Bostock H & Vogel W (1999). Human axons contain at least five types of voltage-dependent potassium channels. *J Physiol* **518**, 681–696.

Röper J & Schwarz JR (1989). Heterogeneous distribution of fast and slow potassium channels in myelinated rat nerve fibres. *J Physiol* **416**, 93–110.

Rundfeldt C (1997). The anticonvulsant retigabine (D-23129) acts as an opener of $K^+$ channels in neuronal cells. *Europ J Pharmacol* **336**, 243–249.

Rundfeldt C & Netzer R (2000). The novel anticonvulsant retigabine activates M-currents in Chinese hamster ovary-cells transfected with human KCNQ2/3 subunits. *Neurosci Lett* **282**, 73–76.

Safronov BV, Kampe K & Vogel W (1993). Single voltage-dependent potassium channels in rat peripheral nerve membrane. *J Physiol* **460**, 675–691.

Scherer SS, Arroyo EJ & Peles E (2004). Functional organization of the nodes of Ranvier. In *Myelin Biology and Disorders*, ed. Lazzarini RA, Griffin JW, Lassman H, Nave K-A, Miller R & Trapp B, pp. 89–116. Elsevier, San Diego.

Schmalbruch H (1986). Fiber composition of the rat sciatic nerve. *Anat Rec* **215**, 71–81.

Schroeder BC, Kubisch C, Stein V & Jentsch TJ (1998). Moderate loss of function of cyclic-AMP-modulated KCNQ2/KCNQ3 K channels causes epilepsy. *Nature* **396**, 687–690.

Schwarz JR, Reid G & Bostock H (1995). Action potentials and membrane currents in the human node of Ranvier. *Pflugers Arch* **430**, 283–292.

Selyanko AA, Hadley JK & Brown DA (2001). Properties of single M-type KCNQ2/KCNQ3 potassium channels expressed in mammalian cells. *J Physiol* **534**, 15–24.

Selyanko AA, Hadley JK, Wood IC, Abogadie FC, Jentsch TJ & Brown DA (2000). Inhibition of KCNQ1–4 potassium channels expressed in mammalian cells via M1 muscarinic acetylcholine receptors. *J Physiol* **522**, 349–355.

Shen W, Hamilton SE, Nathanson NM & Surmeier DJ (2005). Cholinergic suppression of KCNQ channel currents enhances excitability of striatal medium spiny neurons. *J Neurosc* **25**, 7449–7458.

Singh NA, Charlier C, Stauffer D, DuPont BR, Leach RJ, Melis R, Ronen GM, Bjerre I, Quattlebaum T & Murphy JV (1998). A novel potassium channel gene, KCNQ2, is mutated in an inherited epilepsy of newborns. *Nat Genet* **18**, 25–29.

Stämpfli R & Hille B (1976). Electrophysiology of the peripheral myelinated nerve. In *Frog Neurobiology*, ed. Llinás R & Precht W, pp. 3–32. Springer Verlag, Berlin Heidelberg.

Tatulian L, Delmas P, Abogadie FC & Brown DA (2001). Activation of expressed KCNQ potassium currents and native neuronal M-type potassium currents by the anti-convulsant drug retigabine. *J Neurosci* **21**, 5535–5545.

Vleggeert-Lankamp CL, Van den Berg RJ, Feirabend HK, Lakke EA, Malessy MJ & Thomeer RT (2004). Electrophysiology and morphometry of the A$\alpha$- and A$\beta$-fiber populations in the normal and regenerating rat sciatic nerve. *Exp Neurol* **187**, 337–349.

Vogel W & Schwarz JR (1995). Voltage-clamp studies in axons: macroscopic and single-channel currents. Action potentials and nodal membrane currents. In *The Axon*, ed. Waxman JD, Kocsis JD & Stys PK, pp. 257–280. Oxford University Press, Oxford.

Wang H-S, Pan Z, Shi W, Brown BS, Wymore RS, Cohen IS, Dixon JE & McKinnon D (1998). KCNQ2 and KCNQ3 potassium channel subunits: molecular correlates of the M-channel. *Science* **282**, 1890–1893.

Wickenden AD, Yu W, Zou A, Jegla T & Wagoner PK (2000). Retigabine, a novel anti-convulsant, enhances activation of KCNQ2/Q3 potassium channels. *Mol Pharmacol* **58**, 591–600.

Yang Q, Kaji R, Hirota N, Kojima Y, Takagi T, Kohara N, Kimura J, Shibasaki H & Bostock H (2000). Effect of maturation on nerve excitability in an experimental model of threshold electrotonus. *Muscle Nerve* **23**, 498–506.

## Acknowledgements

We thank Dr Christiane K. Bauer for helpful comments on the manuscript and Dr Dirk Isbrandt for his continuous interest and the supply of XE991. Supported by US National Institutes of Health R01 NS49119 and a Miles Family Fund Clinician-Scholar Award (to E.C.C.).